EUROPEAN SPALLATION SOURCE

2014/2015 Round Instrument Construction Proposal
Revision Date 25/04/2019

Expression of Interest for
A New Search for Neutron-Anti-Neutron Oscillations at ESS

European Spallation Source ESS AB
Visiting address: ESS, Tunavägen 24
P.O. Box 176
SE-221 00 Lund
SWEDEN

www.esss.se

EUROPEAN SPALLATION SOURCE

2014/2015 Round Instrument Construction Proposal
Revision Date 25/04/2019

	Name	Affiliation
Main proposer	Gustaaf Brooijmans	Columbia University
Co-proposers	David Baxter	Indiana University
	Lorenzo Calibbi	Université Libre de Bruxelles
	Luis Castellanos	University of Tennessee
	Joakim Cederkäll	Lund University
	Brian Cole	Columbia University
	Gabriele Ferretti	Chalmers University of Technology
	Peter Fierlinger	TU Munich
	Matthew Frost	University of Tennessee
	Franz Gallmeier	University of Tennessee, Oak Ridge National Laboratory
	Kenneth Ganezer	California State University Dominguez Hills
	Richard Hall-Wilton	ESS
	Lawrence Heilbronn	University of Tennessee
	Go Ishikawa	Nagoya University
	Tord Johansson	Uppsala University
	Leif Jönsson	Lund University
	Yuri Kamyshkov	University of Tennessee
	Masaaki Kitaguchi	Nagoya University
	Esben Klinkby	ESS
	Mats Lindroos	ESS
	Bernhard Meirose	University of Texas Dallas
	David Milstead	Stockholm University
	Rabindra Mohapatra	University of Maryland
	Thomas Nilsson	Chalmers University of Technology
	Anders Oskarsson	Lund University
	Robert Pattie	Los Alamos National Laboratory
	Christoffer Petersson	Chalmers University of Technology
	David Phillips	North Carolina State University
	Amlan Ray	VECC, Kolkata, India
	Filippo Resnati	CERN
	Arthur Ruggles	University of Tennessee
	Utpal Sarkar	Physical Research Laboratory, Ahmedabad, India
	Alexander Saunders	Los Alamos National Laboratory
	Hirohiko M. Shimizu	Nagoya University
	Robert Shrock	Stony Brook University
	Samuel Silverstein	Stockholm University
	Camille Theroine	ESS
	Lawrence Townsend	University of Tennessee
	Rick Van Kooten	Indiana University
	Albert Young	North Carolina State University
ESS coordinator	Camille Theroine	ESS

Note: All proposals received by ESS will be included as Expressions of Interest for In-kind contributions. ESS will use this information for planning purposes and the proposer or affiliated organization is not obligated to materially contribute to the project.

European Spallation Source ESS AB
Visiting address: ESS, Tunavägen 24
P.O. Box 176
SE-221 00 Lund
SWEDEN

www.esss.se

The following table is used to track the ESS internal distribution of the submitted proposal.

	Name	**Affiliation**
Document reviewer	Ken Andersen	ESS
Distribution	Dimitri Argyriou, Oliver Kirstein, Arno Hiess, Robert Connatser, Sindra Petersson Arskold, Richard Hall-Wilton, Phillip Bentley, Iain Sutton, Thomas Gahl, relevant STAP	ESS

European Spallation Source ESS AB
Visiting address: ESS, Tunavägen 24
P.O. Box 176
SE-221 00 Lund
SWEDEN

www.esss.se

EXECUTIVE SUMMARY

A sensitive search for neutron-antineutron oscillations can provide a unique probe of some of the central questions in the particle physics and cosmology: the energy scale and mechanism for baryon number violation, the origin of the baryon-antibaryon asymmetry of the universe (with implications for static electric dipole moments), and the mechanism for neutrino mass generation. The decay of a proton (or of a neutron that is otherwise stably bound in a nucleus) is an obvious candidate for baryon number violation studies, violating baryon number by 1 unit, $\Delta B = 1$, and current limits probe very high energy scales ($\sim 10^{15} - 10^{16}$ GeV). Neutron-antineutron oscillations, on the other hand, violate baryon number by 2 units, and can take place even if proton decay is absent. They can be induced by new physics at energy scales as low as a few TeV. In fact, some models which predict $n \to \bar{n}$ oscillations also predict measurable signatures (due to "colored scalars") within reach of the Large Hadron Collider. Neutron-antineutron oscillations provide an experimentally accessible window on a variety of sources of new physics at moderate energy scales, such as theories with extra spatial dimensions and viable models for baryogenesis at or below the electroweak symmetry-breaking scale. The $\Delta B=2$ selection rule relates $n \to \bar{n}$ oscillations to Majorana neutrino mass generation in models which unify quarks and leptons, providing another window on the origin of neutrino mass.

Given the connections to these essential questions, the unambiguous detection of $n \to \bar{n}$ oscillations would have enormous impact on the course of particle physics, not only motivating improvements in the detection sensitivity, but establishing new physics at accessible energy scales. Experiments designed to detect $n \to \bar{n}$ oscillations fall into two categories: large volume, low background underground experiments and experiments with cold neutrons. In both cases, the experimental signature that an oscillation has taken place is striking: the annihilation of the antineutron, releasing roughly 2 GeV of energy, typically in the form of pions (4 to 5 pions on average). At present, the best limits on $n \to \bar{n}$ oscillations come from water Cerenkov detectors (SuperKamiokande), where limits are derived from oscillations for neutrons bound in oxygen nuclei. These experiments, however, are already limited by an irreducible background from atmospheric neutrinos, making large increments in sensitivity prohibitively difficult. Experiments with cold neutron beams do not suffer from this limitation, in that the oscillation amplitude develops "in-flight" as a cold neutron beam propagates freely from a focusing optic to an annihilation target. The target is surrounded by a detector capable of accurately reconstructing the annihilation vertex position and release energy, providing essentially background free detection of the annihilation signature. The most sensitive cold neutron experiment to date was performed at ILL in 1990, and is about three times less sensitive to antineutron annihilations than the SuperKamiokande experiment. With the advances in neutronics technology over the last 25 years, a new cold neutron experiment can now be performed with a very large increase in sensitivity.

A remarkable opportunity has emerged to pursue this objective with the construction of the European Spallation Source (ESS). The envisioned experiment's goal is to have at least a factor of 1000 greater sensitivity to the oscillation probability than the ILL experiment (after 3 years of operation). The critical technologies (advanced neutron optics and high resolution trackers and calorimeters) already exist, and the ongoing work towards a technical proposal is focused on a cost-effective optimization of the experiment.

TABLE OF CONTENTS

1. INSTRUMENT PROPOSAL

1.1 Scientific Case

A true understanding of the physics of baryon number violation would require comprehensive knowledge of the underlying symmetry principles, with distinct selection rules corresponding to different complementary scenarios for unification and for the generation of baryon asymmetry of the universe [1]. Thus, discovery of proton decay with the selection rule $\Delta B = 1$ would imply the existence of new physics at an energy scale of $10^{15} - 10^{16}$ GeV, while discovery of $n \to \bar{n}$ oscillation with the selection rule $\Delta B = 2$ would point to new physics near or above the TeV scale [2]. There also exist many models, including those with extra space dimensions at the TeV scale [3], with local or global B or $B-L$ symmetry that do not allow proton decay, and where $n \to \bar{n}$ oscillation (transformation) is the only observable baryon number violating process [4].

The discovery of neutrino mass provided the first direct evidence for physics beyond the Standard Model. A simple way to understand the small neutrino masses is by the seesaw mechanism [5-9], in which the neutrino is a Majorana fermion, i.e., it breaks lepton number L by two units. However, even if the Majorana nature of the neutrino is established through observation of neutrinoless double beta decay, we still need to understand at what scale the dynamics occurs. Although neither B nor L is gauged in the Standard Model (SM) or in the SU(5) grand unified theory (GUT), there are extensions of the SM where B and L are gauged (in the combination B-L to remain anomaly-free), such as the left-right symmetric model with gauge group $SU(3)_c$ x $SU(2)_L$ x $SU(2)_R$ x $U(1)_{B-L}$ and the SO(10) GUT. In these extensions, if L is broken by two units, as it is with Majorana neutrino mass terms, then it is natural for B to be broken by two units as well.

Indeed, quark-lepton unified theories that predict Majorana neutrinos also predict $n \to \bar{n}$ oscillations. The search for $n \to \bar{n}$ oscillations will therefore complement neutrinoless double beta decay experiments in elucidating UV extensions of the Standard Model that predict both ΔL=2 and ΔB=2 processes. In particular, an observation of $n \to \bar{n}$ oscillation may indicate that the small neutrino mass is not a signal of physics at the GUT scale but rather a much lower scale, possibly not too far above a TeV. A given fundamental theory yields an effective Lagrangian containing six-quark operators O_i that mediate the transition udd to $u^c d^c d^c$ at the quark level. It is then necessary to calculate the matrix elements $\langle n^c | O_i | n \rangle$ of these six-quark operators to obtain predictions for rates to be expected in an experiment and to work back from an experimental limit or observation to constrain parameters in a fundamental theory. These matrix element calculations have been done [10].

Originally it was thought that proton decay predicted by grand unified theories could generate the matter-antimatter asymmetry observed in the universe. However, since sphaleron processes in the Standard Model violate $B+L$ number [11], any $B-L$ conserving GUT-scale-induced baryon asymmetry would be washed out at the electroweak phase transition [12]. The lepton number violating decays of the right-handed neutrino within minimal SO(10)-type GUTs can naturally explain the observed matter-antimatter asymmetry via the process of leptogenesis [13]. Observation of $n \to \bar{n}$ oscillations at currently achievable sensitivity would, however, hint at a new mechanism for the generation of matter-antimatter asymmetry, since the baryon excess generated by leptogenesis would be washed away [12]. It has been shown that the same physics that leads to $n \to \bar{n}$ oscillation also provides a mechanism for baryogenesis at scales below the electroweak phase transition. Existing theories describing such processes typically also predict colored scalars within or just beyond the reach of the LHC, along with an observable electric dipole moment of the neutron and some rare B-meson decay channels [14].

Supersymmetric (SUSY) theories [cite Martin's review? (arXiv:hep-ph/9709356)] provide a well motivated framework in which to investigate baryon number violation. In their most common formulation, SUSY models at the electro-weak scale comprise a symmetry (*R*-parity) that forbids all *B* and *L* violating processes and allows for a Dark Matter candidate of WIMP type. However, the lack of missing energy signatures in the first LHC run has prompted theorist to allow *R*-parity violating (RPV) terms that would weaken the current exclusion limits. (In this scenario Dark Matter could be provided by axion-like particles.) A particular class of RPV models includes interactions that violate *B* but not *L*. Under such condition, (and provided no additional neutral fermion lighter than the proton exists), the proton is still stable but ΔB=2 processes, such as $n \to \bar{n}$ oscillations or di-nucleon decay, are expected to occur. Their rates can be related to other rare phenomena such as meson-antimeson mixing and flavor changing neutral processes. Under some further model-dependent assumption one can also relate the above phenomena to the dynamics of top squark decay.

The probability of $n \to \bar{n}$ transformation in vacuum in the absence of a magnetic field is $P \cong (t/\tau)^2$, where t is the free neutron propagation time in vacuum and τ is a characteristic oscillation time determined by new physics processes that induce $\Delta B = 2$ transformations. If the effective scale of the relevant new physics is around ($10^4 - 10^6$)

GeV, as predicted by various theoretical models, the possible range of $n \to \bar{n}$ oscillation time is $\tau \sim (10^9 - 10^{11})$ seconds [2].

Previous $n \to \bar{n}$ Searches

Transformation of neutrons to antineutrons with neutrons bound inside nuclei has been sought in large underground proton decay and neutrino detectors: for example inside iron by the Soudan-2 experiment [15], and most recently inside oxygen by the Super-Kamiokande experiment [16]. Compared to free neutron transformation in vacuum, the intranuclear $n \to \bar{n}$ transformation is strongly suppressed by the difference of nuclear potential for neutrons and antineutrons. This suppression was calculated using quantum mechanical nuclear theoretical models [17, 18].

An antineutron transformed from the neutron inside the nucleus is expected to annihilate quickly with one of the surrounding nucleons and to produce multiple secondary hadrons, mainly pions that will be available for detection. Experimentally the search for $n \to \bar{n}$ transformation in all the above-mentioned experiments is limited by atmospheric neutrino backgrounds. The best result so far was obtained in the Super-Kamiokande 50-kt water Cherenkov experiment, where 24 $n \to \bar{n}$ candidate events were observed for 1489 exposure days with an estimated atmospheric neutrino background of 24.1 events. Based on this observation, the lower limit on the lifetime for neutrons bound in ^{16}O was calculated to be 1.89×10^{32} years at the 90% CL [16].

The lifetime limit for bound nucleons (τ) in ^{16}O nucleus can be converted to the $n \to \bar{n}$ oscillation time for a free neutron (τ) using the relationship: $T(\text{intranuclear}) = R \cdot \tau^2(\text{free}),$ where R is the nuclear suppression factor [2, 17, 18]. Thus, the corresponding limit for the oscillation time of free neutrons from the Super-K limit can be calculated as 2.44×10^8 s using $R = 1.0 \times 10^{23} s^{-1}$ [17]. For a more recent theoretical model [18] where $R = 0.52 \times 10^{23} s^{-1}$, one can find a limit for the free neutron oscillation time as 3.38×10^8 s.

An alternative approach to the search for $n \to \bar{n}$ oscillations is with free neutrons. This possesses superior background rejection, allows the possibility of turning off the signal using a small magnetic field, and therefore has enormous potential in exploring the stability of matter. Thus, for example, a limit on the free-neutron oscillation time $\tau > 10^{10}$ s would correspond to the limit on matter stability of $T_A = 1.6–3.1 \times 10^{35}$ years [17, 18].

The previous experimental search for free $n \to \bar{n}$ using a cold neutron beam with a flux 1.25×10^{11} *n/s* from the research reactor at the Institute Laue-Langevin (ILL) in Grenoble gave a limit $\tau > 0.86 \times 10^8$ *s* in 1994 [19]. The average velocity of the cold neutrons used was ~700 *m/s* and the average neutron flight time was ~ 0.1 *s*. A vacuum of $P \simeq 2 \times 10^{-4} Pa$ was maintained in the neutron flight volume and the Earth magnetic field was shielded down to $B < 10\ nT$. Antineutron appearance was sought through annihilation in a ~130 μm carbon film target, generating a star pattern of several secondary pions, viewed by a tracking detector, and the energy deposition of a little under two GeV in the surrounding calorimeter. This detection process strongly

suppresses backgrounds. In one year of operation the ILL experiment saw zero candidate events with zero background [19].

1.2 Description of Instrument Concept and Performance

In the case of a cold neutron beam traveling through a vacuum in a magnetic field $\vec{B}$, the energy gap between n and $\bar{n}$ states is given by $\Delta E = 2\vec{\mu}\cdot\vec{B}$. In a new experiment at ESS, the beam of cold neutrons with flight time ≤ 1 sec would traverse a region with high vacuum and ultra-low magnetic field such that the quasi-free condition holds giving $\Delta E \cdot t \ll \hbar$, and the simple equation $P(\bar{n},t) = (t/\tau)^2$ may be used for the $n \to \bar{n}$ transformation probability. This implies the magnetic field must be suppressed to ≤ 5 nT in the whole free flight volume and the vacuum should be better than ~ 10^{-5} Pa.

The figure of merit (or sensitivity) for a free $n \to \bar{n}$ search experiment is $N_n \cdot t^2$, where N_n is the free neutron flux reaching the annihilation target and t is the neutron observation time. A schematic configuration of the ILL experiment [19] is shown in Fig.1. If the neutrons are emitted from the source isotropically with intensity I_0 per steradian the observable neutron flux will be $I_0 A / L^2$, where A is the annihilation target area and L is the distance between source and target. Since $t = L / v_n$, the sensitivity does not directly depend on L, thus an increase of sensitivity can also be achieved by lowering the neutron velocities v_n i.e. with a neutron source thermalized to the lowest possible temperature (~ 35K at ILL). However, with a horizontal layout, as the one shown in Figure 1, a lower limit on the neutron velocity – excluding the use of very cold (< 200 m/s) and ultra-cold neutrons UCN (<7 m/s) – is imposed by Earth's gravity since very slow neutrons cannot be transported over significant distances in the horizontal direction without repeated interactions with a mirror. Such interactions "reset" the oscillation clock. The initial intensity of the neutron source was determined in the ILL experiment by the curved neutron guide (not shown in Figure 1); it was slightly improved by the divergent neutron guide (see Figure 1).

A next-generation experiment at ESS would use a similar configuration as used at ILL, but exploiting progress in both neutronics and detector technologies to push the experiment's sensitivity to the oscillation probability by approximately three orders of magnitude. Essential for the increase of sensitivity is a large elliptical focusing super-mirror reflector that intercepts off-axis cold neutrons from the moderator and directs them by single reflection to the target surrounded by the annihilation detector [20]. A schematic view of the experiment is shown in Figure 2.

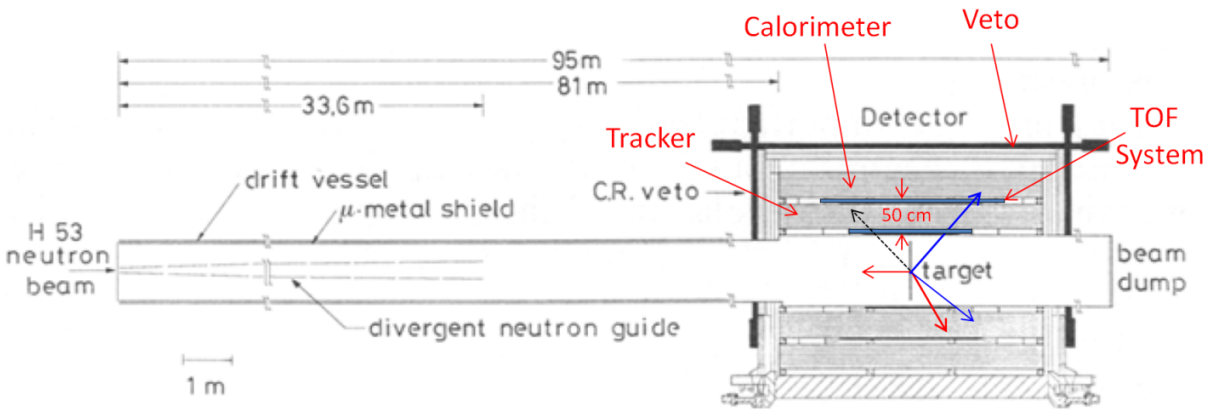

Figure 1: Configuration of 1991 horizontal experiment at the ILL in Grenoble [19].

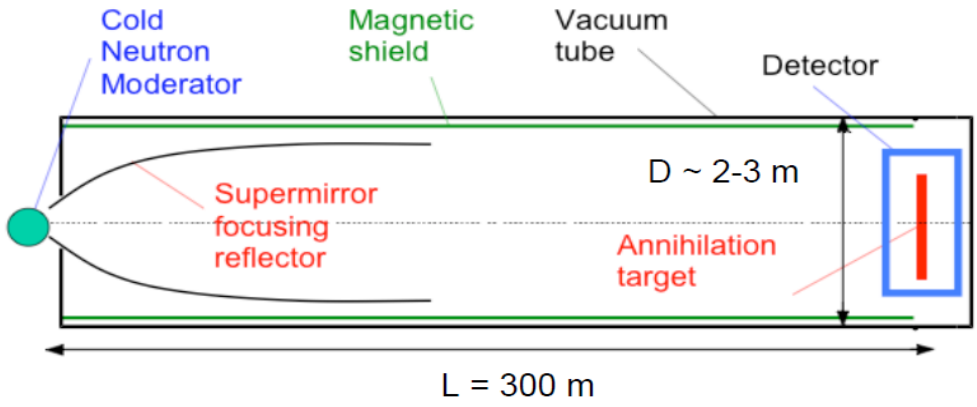

Figure 2: Schematic view of the new experiment with horizontal layout.

Neutronics

The specific sensitivity (figure of merit) $N_n \cdot t^2$ reveals the need for maximization of three characteristics of the ESS experiment/target interface.

(1) A moderator that delivers the highest possible intensity of cold neutrons (energy < 5meV, or velocity < 1000 m/s, or wavelength > 4Å) is important towards improving both N_n and t. The overall intensity is the product of brightness and moderator area, so that maximizing the product of the two is beneficial.

(2) A large beam port allowing the largest possible solid angle view of the cold moderator surface area will ensure that a maximal fraction of the flux will be accessible to the initial reflector geometry, thus enhancing transport to the annihilation target.

(3) An overall lower neutron spectrum emission temperature is desirable from the standpoint of enhancing the transport efficiency of the $m = 6$ super-mirror reflector. This would also boost the sensitivity significantly by increasing the mean transit time. Higher

m technology is under development by the collaboration to further enhance the experiment's sensitivity.

Besides the obvious factors (higher power, larger detector, etc.) the higher sensitivity of a new experiment, as compared to the previous ILL-based experiment, is driven by progress in neutron guiding and particle detection technologies. Neutrons with transverse velocities up to 7 m/s can be 100% mirror-reflected from the surfaces of some materials that possess high Fermi-potentials. Multi-layered surfaces (super mirrors) can enhance the range of reflected transverse velocities by *m*-times due to Bragg scattering. However, the reflection coefficient of super mirrors is not 100% and typically decreases with the transverse velocity due to the roughness of the substrate surface and the accuracy of layer deposition. Super-mirrors to *m=4* are an industrial standard and super-mirrors with up to *m=7* can be industrially produced [21].

To enhance the sensitivity of the $n \rightarrow \bar{n}$ search the super-mirror needs to be optimized to match the moderator geometry. For a simple, point-like source it would be arranged in the shape of a truncated focusing ellipsoid as shown in Figure 3. A focusing reflector with a large acceptance aperture will intercept neutrons within a fixed solid angle and direct them by a single reflection to the target. The cold neutron source and annihilation target will be located in the focal planes of the ellipsoid. Here ZTARG, the distance moderator-detector ≥ 200 m; RTARG, the radius of the annihilation target = 1m; BTUB, the small demi-axis of the elliptical super-mirror reflector ≥ 2 m; the maximum *m*-number of the super-mirror *m*=6; Z_0, the distance from moderator to reflector start ≤ 10 m; Z_m, the distance from moderator to reflector end = 50 m. The source and the target are not point-like objects, however, and the geometry of the reflector and the parameter *m* of the mirror material need to be optimized in order to maximize the sensitivity $N_n t^2$. Figure 4 shows the transport efficiency of a simple ellipsoidal reflector with focal point centred between the two moderators as a function of the point of origin of the neutrons. For neutrons coming from the cold moderators, the efficiency is about 10% of that for neutrons that would be produced at the ellipsoid's focal point.

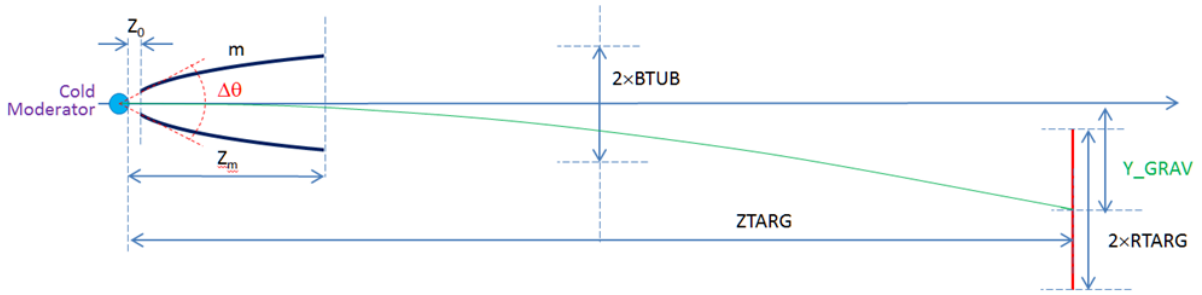

Figure 3: Schematic indicating the preliminary baseline parameters of a new experiment.

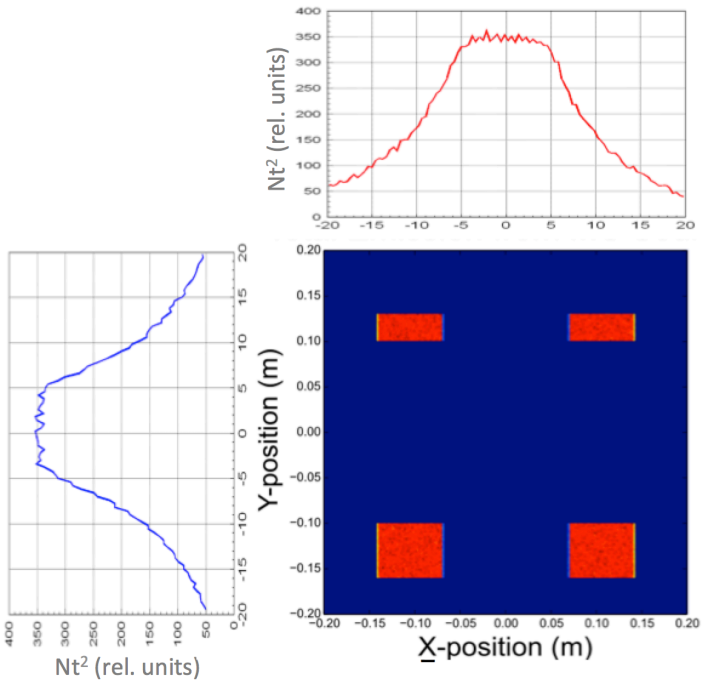

Figure 4: View of the BF-2 moderators from the super-mirror showing the cold moderators in red. The top and left figures show the relative guiding efficiency by a mirror centred on the middle point as a function of the point of emission.

To mitigate this, a "clover" geometry, as shown in Figure 5, is under investigation. This geometry is an assembly of four quarter ellipsoids, each centred on one of the cold moderators. A simpler alternative being studied is a single ellipsoid centred on one of the moderators.

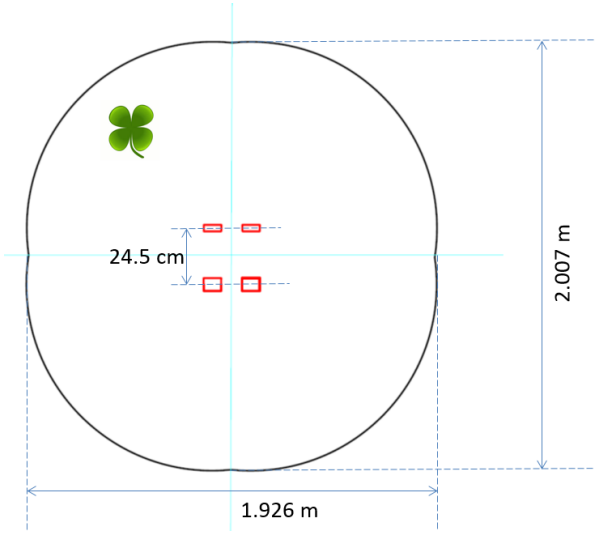

Figure 5: Clover reflector configuration to improve the supermirror efficiency for the two BF-2 moderator configuration.

The moderator area viewed by the experiment is determined in large part by the size of the opening and position of the reflector entrance. The initial position of the beginning of the focusing reflector assumed in the baseline configuration is 10 meters from the moderator, with the opening radius 0.87 meters. This defines an angle that is ±5° (for a total of 10□) from the beam axis. To understand the impact of reflectors and shielding close to the moderators, the experiment's sensitivity is compared for two configurations: one where the neutrons originate at the surface of the BF-2 moderators and are transported through the baseline NNbar configuration including Be reflector and Fe shield and one without those. A configuration with an elliptical supermirror centred between the moderators and no Be and Fe elements gives a sensitivity of 151 ILL units, 114 from the cold source and an additional 37 from the thermal moderator, which delivers many fewer cold neutrons that are transported with much higher efficiency. The Be and Fe elements constrict the solid angle seen by the supermirror and reduce the experiment's sensitivity by a factor 2.25. It would therefore be interesting to study the possibility of enlarging the conical penetration through the Be and Fe, as shown in Figure 6.

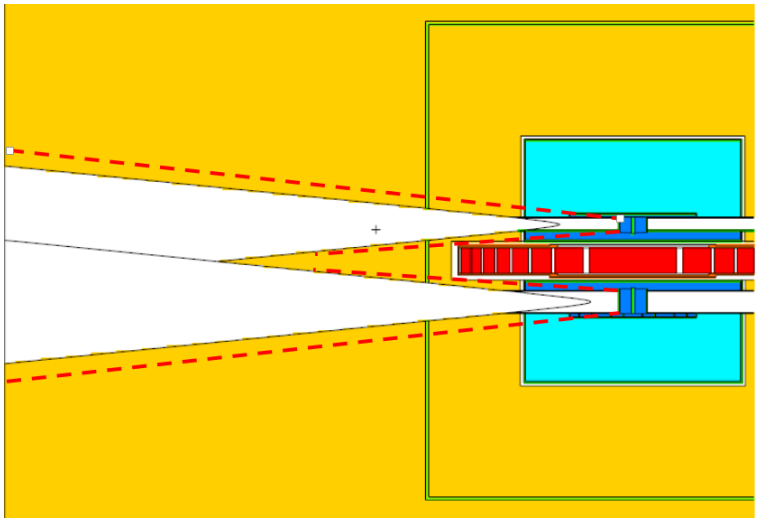

Figure 6: Enlarged (red dashed) conical penetration through the Be reflector and Fe shield.

The results are based on a list of neutrons with complete phase-space information provided by the ESS neutronics group. Ray-tracing simulations through various experiment configurations are performed with this information, and final sensitivity values are presented in units of the ILL experiment's sensitivity.

In addition to challenges associated with the source/reflector interface, compromises will be made with regards to the true geometry of the reflector. The reflector as currently simulated represents a perfect ellipsoid. Given the current state of mirror technology, the optimised reflector will need to be segmented for the sake of feasibility. Preliminary investigations suggest that polygonalization around the beam direction has a more significant impact than along the beam direction.

Provided appropriate shielding around this large beam port is installed to control the background in the hall, the experiment should not impact any decision regarding current or future neutron scattering instrumentation. How that design progresses depends heavily on the final source configuration, and challenges associated with the interface to the proposed experiment. The large beam port that would be required for the experiment can be designed in a way that facilitates easy removal and replacement with an insert appropriate for future neutron instrumentation needs.

If beam lines close to the $n \to \bar{n}$ beam line will use high stray and/or alternating magnetic fields these might negatively impact the magnetic shielding for the experiment and impact its sensitivity. The effect of the experiment's magnetic field compensation system on the neighboring instruments will be minimal since it will compensate the Earth magnetic field of order 0.5 Gauss. The annihilation target and detector positions are much further from the source than other instruments are expected to be (>150 meters), which should allow plenty of room for shielding to prevent cross-talk of any kind between instruments.

The experiment's sensitivity is limited by the solid angle fraction of the neutron beam that reaches the detector. Further improvement of the sensitivity by extending the focusing optics closer to the neutron source is the subject of an R&D program running in parallel with the more standard optics design. The figure of merit $N_n \cdot t^2$ corresponding to the reflection position and m-value of the applied supermirrors is shown in Figure 7. Upstream of the main optics, high-m mirrors are required to gain the FOM. The extended part's geometry will depend on the beamline configuration close to the moderator. The gain obtained by adding optics at 2.6m<z<10m is shown in Figure 7 for two geometries: an ellipsoid and a beaked ellipsoid cut in the horizontal plane. The extension with m=10 supermirrors can increase the figure of merit by 1.6 times. Today m=10-equivalent multilayer mirrors can be fabricated using an ion beam sputtering method. A metal substrate is required for the very difficult radiation environment near the neutron source. Metal substrate machining with surface roughness of 0.4nm, which can be used to effective m~10 mirrors, is under development.

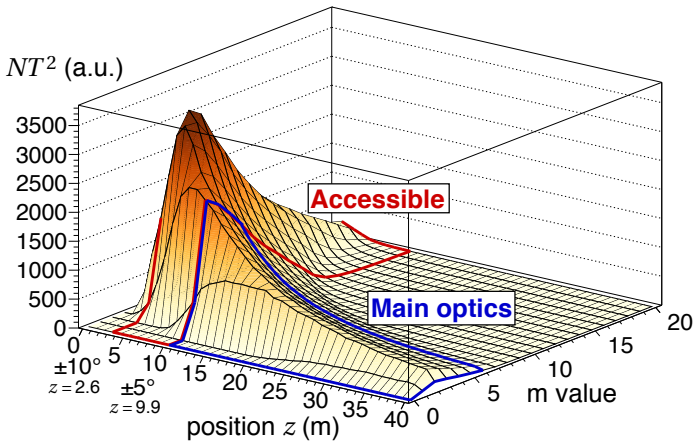

Figure 8a: Reflection position along the beam direction and corresponding m-value for neutrons reaching the detector.

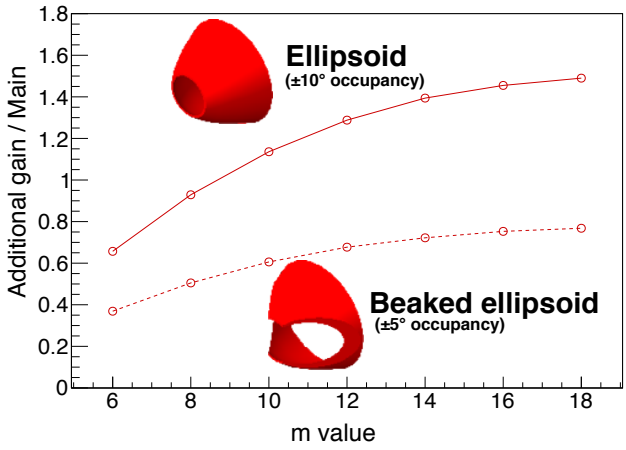

Figure 7b: Gain in sensitivity using optics upstream of the main supermirror.

Magnetics

The experiment will require a vacuum of 10^{-5} mbar and magnetic field of $B \leq 5$ nT along the flight path of the neutrons. The target vacuum is achievable with a vacuum chamber made from highly non-magnetic metals, like aluminum, and pumping of the vacuum can be done using turbo-molecular pumps, which are mounted outside the magnetic shielding. Aluminum is in addition a favorable material for neutron transmission at the entrance into the vacuum-chamber and has low activation. A closed aluminum volume also provides RF shielding, which is relevant for magnetic field sensor- and detector operation inside the volume.

The reduction of ambient magnetic fields to a level of ~ 10 nT over large volumes has been demonstrated in the ILL experiment [19]. Further advances have been made using magnetically shielded rooms (MSRs). Here, the BMSR-II facility has set the scale over the last decade, with a field of < 2 nT over 1 m^3 in a total inner volume of 2.9 x 2.9 x 2.9 m and a damping factor of 75.000 of 1 μT distortions at 10 mHz [22]. Recently, the magnetic shield of the neutron EDM experiment at TU München has achieved a residual magnetic field of 0.3 nT over 1 m^3, with overall inner dimensions variable from a small volume 1.5 x 1.5 x 2.2 m to a large volume of 2.3 x 2.5 x 2.8 m [23, 24]. In the latter case, the fraction of the volume containing a low field was massively improved compared to the previous state-of-the-art setups. Whereas the damping factor of external distortions at low frequencies using the small inner volume is 10^6, the damping factor in the case of the large volume is only 270, but without losing the quality of the residual field.

The residual field is thus almost independent of the shielding factor. In addition, an improved technique to magnetically equilibrate the shield in its environment has been developed and applied in MSRs, which results in a (more than one) order of magnitude faster magnetic equilibration procedure and an average residual magnetic field decreased by a factor of three compared to the previous state-of-the-art devices. Sequential magnetic equilibration of segments of the passive shield is currently being investigated on a small-scale prototype.

For the $n \rightarrow \bar{n}$ experiment, a new shielding concept based on the above findings is suggested. It consists of: (i) an aluminum vacuum chamber; (ii) a two-layer passive magnetic shield made from magnetizable alloy with an approximate cylindrical cross section, mounted concentrically around the vacuum chamber with open ends; (iii) end sections made from a combination of passive and active components. This is shown in Figure 8. While there is no technological problem in achieving the target magnetic field, a campaign to optimize the cost will guide the detailed design.

To obtain a residual field of < 5 nT in the whole volume, the passive shield must be sufficiently strong to shield the quasi-static ambient magnetic field. A shield using 2 layers of 2 x 1 mm thick metal sheets with about 25 cm separation for an approximate diameter of 3.5 m with a transverse damping factor of 50-100 will be sufficient. The field inside the shield will be dominated by the magnetization of the inner shield layer, which can be removed by magnetic equilibration to the < 5 nT level. To obtain

acceptably small currents for equilibration, the shield will be equilibrated in multiple segments. Induced remanent fields from the equilibration procedure can be compensated using shielding material mounted at the boundaries of the sections. The performance of this concept has been demonstrated on a small scale but requires a larger scale prototype test. Distortions from outside, e.g. by a moving crane or car, with typically few μT amplitude, will lead to short distortions, which lower the duty cycle of the low-field measurement by few percent and do not cause permanent changes to the residual field. Larger distortions may require repeated magnetic equilibration of selected sections, also reducing the duty-cycle. Such periods may actually turn out to be valuable to the experiment, as no oscillation should be observed at those times. Longitudinal distortions are shielded by a combination of passive shielding (magnetizable material) and active shielding. Active shielding is provided by coils at the detector side of the shield outside of the shield. The coils reduce the static residual field at the position of the end of the passive shields and use feedback from fluxgate-probes to compensate for changes in the ambient field, which would otherwise penetrate the open end of the passive shield.

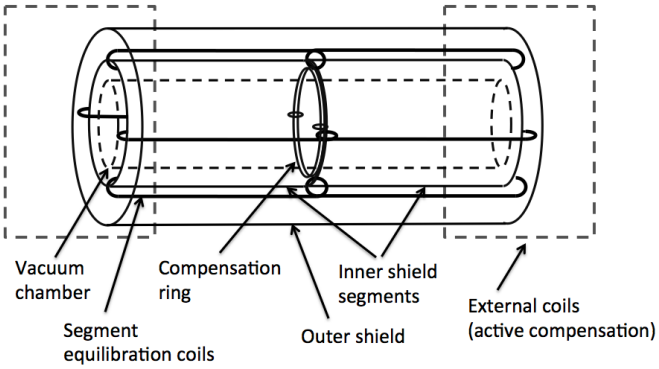

Figure 8: Basic shielding concept: transverse shielding is provided by 2 layers of magnetizable material, longitudinal shielding is provided by a combination of passive and active shielding with measurements at the axial ends of the shield. The vacuum chamber is placed concentrically inside the shield.

An optimization to minimize the effort required for shielding at the end sections will still be required, including adding passive shield strips with large transmission in both ends of the shields. Distortions above 1 Hz frequency are very well shielded by the vacuum-chamber. Access to the vacuum chamber during operation is provided by a sufficiently large number of flanges with less than 30 cm diameter. Off-line access is provided by detachable metal sheets of the passive shields, which can be removed to gain access to larger maintenance-flanges in the vacuum chamber.

Measuring the residual field will be done using fluxgate magnetometers, which provide low drifts and absolute calibration precision of better than 300 pT over many hours. Limited temperature stability and mechanical eigenfrequencies of the static structure may lead to jumps in the residual field of up to few 100 pT, which is not critical for $n \to \bar{n}$. Such systems have been tested and are already operational, e.g. for the measurements in Ref. [23].

Detector

The detector needs to detect the presence of antineutrons in the beam with high efficiency while keeping the background level extremely low. The detection strategy is the same as used in the ILL experiment: antineutron annihilation in a target that is as transparent as possible to neutrons will lead to the production of three or more pions, with an average of five. The detector needs to reconstruct the pion momenta as accurately as possible, as the primary discriminating variables is the multi pion-system invariant mass after establishing the pions come from a common annihilation vertex.

The major subsystems of the annihilation detector (radially in the outward direction - see Fig. 1) are: (i) the annihilation target, (ii) the detector vacuum region inside the vacuum tube, (iii) the tracker, (iv) the time of flight system, (v) the calorimeter, (vi) the cosmic veto system and (vii) the trigger system. Requirements for these subsystems are formulated below. In general, the $n \to \bar{n}$ detector performance is well within current particle detector capabilities, but maximizing acceptance implies it will be large, and a careful cost versus performance optimization will be needed. The detector should be built along the detector vacuum region (see Fig.1) with several layered detection subsystems (sections (iii) - (vi)) and cover a significant solid angle (θ coverage from ~ 20° to 160° corresponds to a solid angle coverage of ~ 94%). In the ϕ projection, the detector configuration can be cylindrical, octagonal, hexagonal, or square as for the ILL experiment.

(i) Annihilation Target. A good option is a uniform carbon disc with a thickness of ~ 100 μm and diameter ~ 2 m. It will be stretched on a low Z-material ring and installed in the center of the detector vacuum region. The material choice is driven by low capture cross section for thermal neutrons ~ 4 mb and high annihilation cross-section ~ 4 kb. In the carbon film the fraction of hydrogen should be below ~ 0.1% to limit generation of capture γ's. Other materials will be evaluated, as well as the possibility of having multiple discs one behind the other, which should allow a data-driven background estimation.

(ii) Detector Vacuum Region. The detector vacuum region will be a tube with inner diameter ~ 2.5 m and wall thickness ~ 1.5 cm. The wall should be made of low Z material (e.g. Al) to reduce multiple scattering for tracking and provide a low (n,γ) cross section. Additional lining of the inner surface of the vacuum region with ^{6}LiF pads will reduce the generation of γ's by captured neutrons. The detector vacuum region is expected to be the source of ~ 10^8 γ's per second originating from neutron capture. Unlike in the neutron beam flight vacuum region, no magnetic shielding is required inside the detector vacuum region. The vacuum level should be 10^{-5} Pa via connection with the neutron beam vacuum region.

(iii) Tracker. Accurate reconstruction of the annihilation vertex position is crucial in background rejection, as it affects the resolution on the invariant mass calculation and overall event momentum balance, and allows suppression of candidates resulting from single particles originating from nearby locations. The tracker is expected to extend radially from the outer surface of the detector vacuum tube by ~ 50 cm and have solid angle coverage of ~ 20°-160°. While the exact specifications will be refined using more detailed simulation, the rms accuracy on the annihilation vertex position will probably be

of order 1 cm, compared to 4 cm in ILL experiment. Candidate tracker technologies include straw tubes, honeycomb chambers and time projection chambers. If there is substantial gain in moving the tracker inside the detector vacuum region for improved accuracy, then the requirements on the detector tube material and thickness will be revisited. Such an approach would impose more stringent constraints on the choice of technology.

(iv) Time of Flight System. A time of flight system (TOF) will serve to suppress background induced by cosmic rays, as well as candidates resulting from single particles originating from nearby locations but slightly different times. The TOF will consist of two layers of fast detectors (e.g. plastic scintillation slabs or tiles) before and after the tracker with solid angle coverage of ~ 20°-160°. With appropriate segmentation, the TOF can provide directional information for all tracks found in the tracker.

(v) Calorimeter. The calorimeter needs to accurately measure photon and pion energies to reconstruct each candidate annihilation event's invariant mass and momentum balance. It will provide trigger signal and energy measurements in the solid angle ~ 20°-160°. The average multiplicity of pions in annihilation at rest is five, so an average pion can be stopped in ~20 cm of dense material (like lead or iron). For contain low multiplicity (but small probability) annihilation modes, the amount of material needs to be slightly be larger. Calorimeter technology options include lead-scintillating fiber "spaghetti" or lead-glass. The detailed performance for the measurement of total energy of annihilation events and momentum balance in θ- and ϕ-projections will be determined from simulations and the technology choice will be made accordingly.

(vi) Cosmic Veto System. The cosmic veto system will identify all cosmic ray background. It will likely be made of large plastic scintillator pads, and can possibly be recycled from existing experiments (Double Chooz, Opera, …) Timing information can potentially be used to supplement the TOF.

(vii) Trigger System. The ILL experiment already observed high single hit rates, so a somewhat more complex trigger system will be required. The advances in FPGA technology will make it possible to use all channels of all subdetectors in the trigger, and track and cluster reconstruction algorithms can be implemented. This will allow a highly selective trigger system to collect both signal and background control samples.

Timing

The flight time from the moderator to the annihilation target will be between 0.1 and 1s, with the slower neutrons contributing more to the experiment's sensitivity. The pulsed nature of the ESS will thus be of limited use for the oscillation signal itself. A substantial number of fast neutrons are expected synchronously with the accelerator pulse however, and these will be used for multiple purposes, including background monitoring and detector timing.

1.3 Technical Maturity

For all the components of the experiment, from the neutron guides to the vacuum tube, magnetic shielding and detector, the technologies are rather well understood. There is no technological risk. However, many choices remain to be made, among which some key items are:

- Geometry and structure of the super-mirror: what will the exact geometry of the mirror be, how will it be segmented for manufacturability, and how will m-values of different segments depend on location?
- How will the magnetic shield be segmented to maximize reusability?
- Which technologies will be chosen for the tracker and calorimeter?

The choices will be made based on extensive simulations that will allow optimization of cost versus sensitivity. These simulations are starting, but they are not sufficiently advanced to make any definite statements.

The expectation is that (groups of) collaborating institutions will take responsibility for the final design and manufacture of different elements of the experiment, and will contribute these in-kind, as is done in most particle physics experiments. The collaboration is currently forming, with the goal to write a Technical Design Report within two years. This would allow for a start of construction around 2018, and commissioning of the experiment soon after first beams are produced by ESS.

1.4 Costing

Given the number of choices that remain to be made, any cost estimate made at this time has a very large uncertainty. Cost will receive significant weight when optimizing the experiment.

The cost drivers are the super-mirror, the magnetic shield and the detector. Order of magnitude estimates indicate that the total cost will be of order 100 million euro, but the uncertainty is at least 50%.

1.5 Timeline

The timeline currently agreed on by the collaboration has the following milestones:

- 2017: Technical Design Report finalized
- 2019: Construction start
- 2022: Commissioning
- 2023-2025: Physics run
- 2026: Dismantling

This timeline is success-oriented but appears feasible, and matches the current ESS plans well, as the physics run will be simultaneous with the ESS initial user program.

2. CONCLUSION

The observation of neutron-anti-neutron oscillations would be a major breakthrough in physics: it would constitute the first observation of baryon number violation, and give a unique insight into Beyond-the-Standard-Model physics. The construction of ESS, together with technological progress, opens the opportunity to conduct a new search for this process

with at least three orders of magnitude increase in sensitivity to the oscillation probability compared to the existing limit from free neutron searches. Such opportunities should not be wasted.

The required technologies exist, and detailed simulations to optimize the designs and technical choices are being developed by a growing collaboration. These should lead to a Technical Design Report in approximately two years, in time to allow the experiment to start taking data not long after ESS starts producing cold neutrons.

3. REFERENCES

[1] K.S. Babu, E. Kearns, U. Al-Binni, S. Banerjee, D.V. Baxter *et al.,* arXiv:1311.5285 (2013).

[2] R.N. Mohapatra, J. Phys. **G36** (2009) 104006, arXiv:0902.0834.

[3] S. Nussinov and R. Shrock, Phys. Rev Lett. **88** (2002) 171601, arXiv:hep-ph/0112337.

[4] J. M. Arnold, B. Fornal, M. B. Wise, Phys. Rev. **D87** (2013) 075004.

[5] P. Minkowski, Phys. Lett. **B67** (1977) 421.

[6] T. Yanagida, Workshop on unified theories and baryon number in the universe, ed. by A. Sawada and A. Sugamoto (KEK, Tsukuba, 1979).

[7] S. Glashow, Quarks and leptons, Cargèse 1979, ed. M.Levy, Plenum (1980).

[8] M. Gell-Mann, P. Ramond and R. Slansky, in "Supergravity", ed. by P. Van Nieuwenhuizen and D. Freeman, North Holland (1980).

[9] R. N. Mohapatra and G. Senjanović, Phys. Rev. Lett. **44** (1980) 912.

[10] S. Rao and R. E. Shrock, Phys. Lett. **116B** (1982) 238; Nucl. Phys. **B232** (1984) 143.

[11] V. Kuzmin, V. Rubakov and M. Shaposhnikov, Phys. Lett. **B155** (1985) 36;

[12] K. S. Babu, R. N. Mohapatra and S. Nasri, Phys. Rev. Lett. **97** (2006) 131301.

[13] M. Fukugita and T. Yanagida, Phys. Lett. **B174** (1986) 45.

[14] K. S. Babu, P. Bhupal Dev, and R. N. Mohapatra, Phys. Rev. **D79** (2009) 015017 and to appear.

[15] J.Chung *et al.*, Phys.Rev. **D66** (2002) 032004.

[16] K. Abe *et al.* [Super-Kamiokande Collaboration], arXiv:1109.4227 [hep-ex].

[17] C. Dover, A. Gal, and J.M. Richard, Phys. Rev. **D27** (1983) 1090.

[18] E. Friedman and A. Gal, Phys. Rev. **D78** (2008) 16002.

[19] M. Baldo-Ceolin *et al.,* Z. Phys. **C63** (1994) 409.

[20] Y. Kamyshkov *et al.*, Proceedings of the ICANS-XIII meeting of the International Collaboration on Advanced Neutron Sources, PSI, Villigen, Switzerland, October 11-14, p. 843 (1995).

[21] Industrial manufacturer of super-mirrors "Swiss Neutronics": http://www.swissneutronics.ch/

[22] J. Bork, H. D. Hahlbohm, R. Klein, A. Schnabel, Biomag2000, Proc. 12th Int. Conf. on Biomagnetism, Finland (2001) 970.

[23] I. Altarev *et al.,* Rev. Sci. Instr. **85** (2014) 075106.

[24] A large scale magnetically shielded environment with 10^6 damping at milli-Hertz frequencies, I. Altarev *et al.,* (unpublished draft)